Enhance hydrogen sulfide (H₂S) gas sensor based on metal oxide semiconductor (NiO) thin films

Radhiyah M Aljarrah and Nawar R A
Department of Physics, Faculty of Science, Kufa University, Najaf, Iraq

E-mail: radhiyah.aljarrah@uokufa.edu.iq

Abstract
The morphological and structural properties of NiO films have been studied to find out the possibility of exploit (exploiting) it as a gas sensor. The thin film of the nickel oxide has been obtained by a chemical spray pyrolysis technique on glass substrates using various concentrations of nickel nitrate hexahydrate [Ni(NO$_3$)$_2$:6H$_2$O] aqueous solution. The produced films were characterized using X-Ray diffraction and atomic force microscopy. The investigations revealed that the crystal structure are a cubic polycrystalline with preferential orientation along the (111) plane. The topographical analyse (AFM) shows that the values of the grain size increasing with increase the concentration, where average of the grain diameter raised from 42.04-110.058 nm of 0.01 M and 0.1M concentrations respectively. The gas sensing results demonstrate that sensitivity of nickel oxide semiconductor films to the hydrogen sulfide gas are affected by the size of the growing crystallites and the operating temperature.

Keywords: AFM, gas sensor, metal oxide semiconductor, operating temperature, sensitivity.

1. Introduction

Oxide semiconductor has made significant development over the past decade, and getting widespread use in various applications including gas sensors. Nickel oxide (NiOx), is a one of many metal oxides materials owning a wide band gap in range of 3.4eV to 3.58eV, and behaves as a p-type semiconducting. Moreover, NiO has high stability in atmospheric conditions and high-temperature resistance [1-3].

However, use in other applications such as medical fields, industry, and harsh environments still requires further development, in terms of sensitivity, selectivity, detection limit and speed of response/recovery times. Nowadays, much effort is directed towards improving the performance of the gas sensor that based on metal oxides semiconductor [4].

In particular, the flexibility of the electronic properties of these materials against mechanical deformation or degradation has made metal oxide semiconductors leading materials of choice for flexible electronics based on elastomeric substrates [5].

Design and fabrication of gas sensor devices based on metal oxide materials such as NiO, with stable and controlled As well as morphological configurations, have become an advanced work topic due to these novel portable sensors are being widely applied in various fields of technology, such as automotive emission monitoring, biological detection, and homeland security. Most works on oxide semiconductor applications have focused on n-type [6]. P-Type oxides are more difficult due to the valence band maxima are composed of O 2p orbitals that are more localized than the s orbitals in the conduction band. As a consequence, hole mobility becomes lower than electron mobility's, which impacts the performance of hole transport. In spite of these challenges, p-type oxides are still important for a wide range of emerging applications [7].

Among these metal oxides, nickel oxide is natural p-type semiconductors owning high electron transport performance, has been considering as the best candidate for gas sensing devices because of has a good sensitivity, and high compatibility with micromachining [8,9].

The NiO thin films can be deposit using a wide range of techniques, including physical vapour deposition, chemical vapour deposition, and chemical-based solution deposition techniques.

Low cost of the chemical based deposition method makes it appealing option, as well; the recent developments with these methods have led to the ability to deposit at atmospheric pressure and higher throughput [10-12].

In general, the mechanisms of gas sensing via semiconductor materials relevant to an injection/extraction the charges process which occur during the absorbing of the targeted molecules by the sensor surface, which in result change the conductivity of

film. The adsorption of the gas molecules in n-type, lead to capture the free electrons, which in turn raises the voltage barrier. This increase in the voltage barrier height impedes the flow of electrons, and increases the electric resistance of the sensing element. While the absorb gas molecules in p-type leads to drop the resistance [9,10].

There are aspects that still need improvement in this kind of sensor, such as operating temperature, selectivity, and time of response/recovery. A lot of researches are trying to improve these aspects [13].

The operating temperature influences on the chemo-dynamic reaction between the gas molecules-solid that result in impact in the sensor sensitivity. Therefore, operating temperature plays an important role in limitation of the sensor performance, such as selectivity, sensitivity, stability, and recovery and response time [14]. The present work investigates the response speed of the sensor for the low concentrations of detect hydrogen sulfide gas (5%) at the operation temperature of 200 ◦C.

2. Experimental procedure

Nickel nitrate hex hydrate (Ni(NO3)2.6H2O), with purity 99.99% used with different weights (0.29079, 0.87238, 1.445397, 2.03555, and 2.03555 gm) were dissolved separately in the distilled water (100 ml) under stirring for one hours to get clear and homogeneous. The concentrations of the precursor can be calculated using the eq.(1) below[15]:

$$M = \frac{W}{M_W} \times \frac{1000}{V},$$ (1)

where M is represent the molar concentration, W is the weights of nickel nitrate, Mw is the molecular weight of nickel nitrate (182.70gm/mol.), and V represents a volume of the distilled water.

The deposition process was carried out after heating the plate to 420 oC by provides the plate by electric heater to keep the plate temperature precision of ±5◦C in the deposition area.

Intermittent spraying technique (10 sec of spraying followed by 2 min, then pause, 5 ml/h of air flow rate) has applied to deposit a thin film with different concentrations (0.01, 0.03, 0.05, 0.07 and 0.1M) on the hot glass substrate. 250-300 nm thickness film has been deposited during about 30 min of intermittent spraying. The thickness of the deposited samples has been estimated using [15]:

$$t = \frac{\Delta m}{A.\rho},$$ (2)

Whereas A represents the actual area, Δm the difference in weight of the substrate before and after deposition nickel oxide wafer, and ρ represents the density of NiO which is equal to 6.67 gm / cm³.

The phase composition and crystalline structure of the spray-NiO thin films was studied using X-Ray Diffraction(PANalytical   X'Pert Pro device) . Device employs Cu Kα (λ =1.1548 Å), tube current 30 mA, and high voltage 40 kV produces output power in range 1.2 kW, The topographical analysis were investigate with atomic force microscopy (AA3000 Scanning Probe

Microscope SPM, tip NSC35 / AIBS)   (this testes XRD and AFM ara making in University of Tehran in Iran)

The Hydrogen sulfide gas is considering as a one of the most dangerous six gases. It is poisonous, corrosive, and flammable. Moreover there are many sources emits it and pollutes the environment, it is found during the drilling and production of crude oil and natural gas, plus in wastewater treatment and utility facilities and sewers. The gas is produced as a result of the microbial breakdown of organic materials in the absence of oxygen . So, according to all above, monitoring the H2S gas emissions processes is important to control the spread this polluted [16].

A custom built system had used to test the sensing characteristics of the gas sensors, by use gas chamber made of acrylic plastic equipped by 150 watt ceramic heater to control the temperature. The target gas was supplied to the chamber by an air pump, and the concentration of target gas was adjusted via two mass flow meters (MFM), these valves have been sitting to 1000 sccm flow during the sensing tests, as shown in figure 1 (missing dot)

Keithley devise (2400 Source Meter, Keithley, Cleveland, Ohio, USA) has been used to record and measure the electrical resistance of the film. The change in the NiO films resistance because of adsorbing gas molecules translates to electrical signal, which can be calibrated to estimate the concentration of the targeted gas. The measurement set-up is shown in figure 1.

The responsitivity for the p-type semiconductor (NiO) and abbreviated gases (H2S) is given [17-19] :

$$S = \frac{R_g - R_a}{R_a} \times 100\%.$$ (3)

Where R_g and R_a represents the value of the sensor resistance with and before present of the target gas, respectively.

3. Results and discussion

3. 1. XRD results

In figure 2 the peaks of the x-ray analysis that appears at 2θ values; 38.5o, 44.70, and 65.20 which corresponds to (111) , (200) and (220) planes respectively   JCPDS (No.47-1049), confirmed the formation of the polycrystalline with face centred cubic structure (FCC) of the NiO thin films.

No peaks have observed relevant to impurities, while there are weak peaks confirm that the films are textured and the deep of the texturing depended on the concentration of sprayed solution that used. Moreover, there are high peaks which indicates these films mainly consist of the crystalline phase.

The crystallite size (D) for the highest peak (111) at 2θ ~ 37.8° calculated by Debay-Scherrer formula [20]:

$$D = \frac{0.9\lambda}{\beta \cos\theta},$$ (4)

where (β) is the value of the half maximum of full width for the peak at diffraction angle (θ)), and λ is the wavelength of the X-Ray beam.

Table 1. Structural parameters of the spray-deposited NiO thin film at different concentration.

concentration (mol/ L)	2Θ (deg)	a_{exp} (Å)	D (nm)	$\delta \times 10^{16}$ (lines/m^2)	$N \times 10^{17}$ (m^{-2})	$\varepsilon \times 10^{-3}$ (%)	σ_{film}
0.01	37.7	3.575	10.67	98.088	3.40	3.433	-0.799
0.03	37.5	3.595	12.18	74.306	2.24	3.248	-0.756
0.05	37.8	3.566	14.20	49.377	1.21	2.842	-0.661
0.07	37.8	3.566	21.86	20.927	0.335	2.441	-0.568
0.1	37.8	3.566	28.46	12.344	0.151	1.214	-0.283
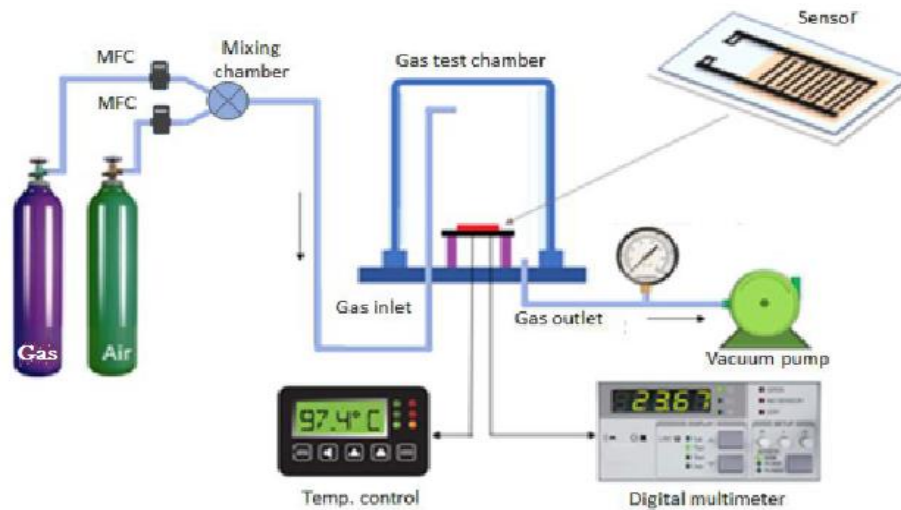
Figure 1. Experiment setup, gas sensor testing system.
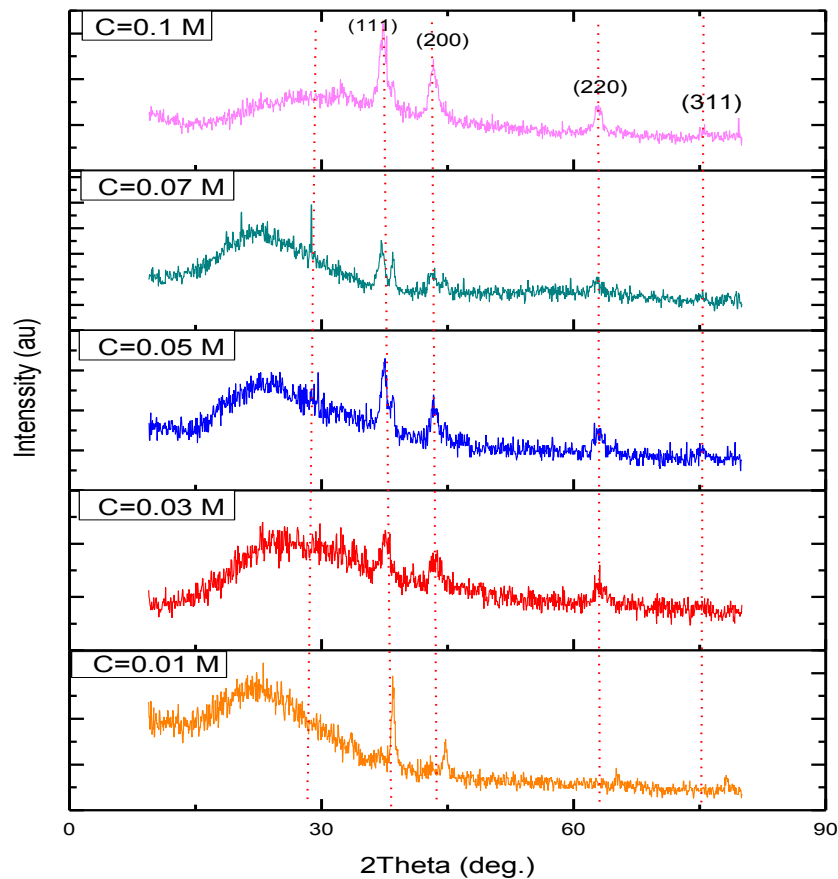
Figure 2. XRD patterns of the spray-NiO thin films at different concentration.
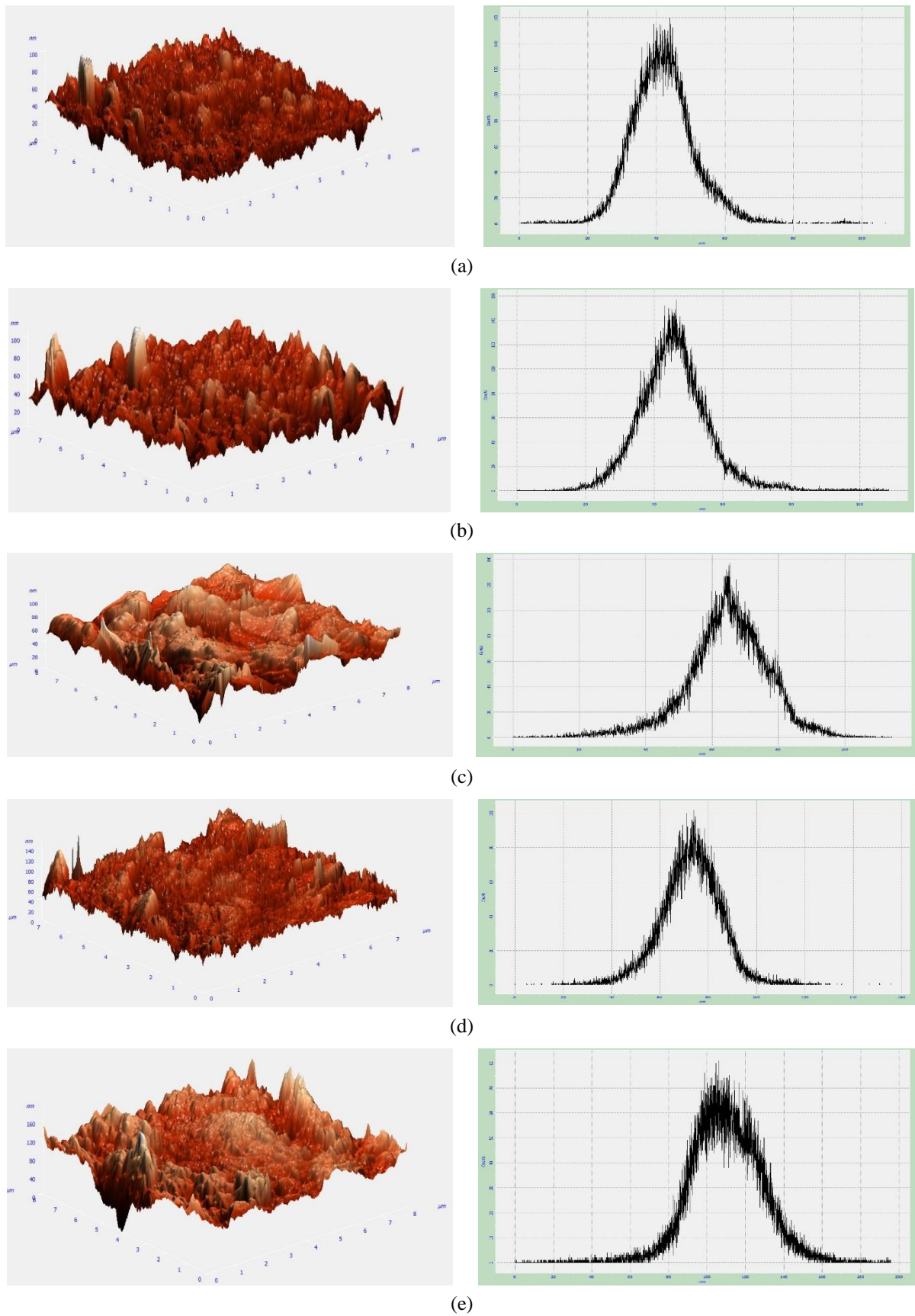
(a)

(b)

(c)

(d)

(e)

Figure 3. AFM images of the spray-deposited NiO thin films at (a:C=0.01 M, b: C=0.03 M,, c: C=0.05 M, d: C=0.07 M, and e: C=0.1 M).

Table 2. Average grain size and roughness for the spray-deposited NiO thin films with different concentration .

Concentration (mol/ L)	Average grain size (nm)	Average Roughness (nm)	Peak-to-peak (nm)
0.01	42.04	6.98789	106.821
0.03	45.733	7.61831	108.356
0.05	64.5739	9.32	114.2
0.07	72.7976	9.53234	155.459
0.1	110.058	14.3348	195.672
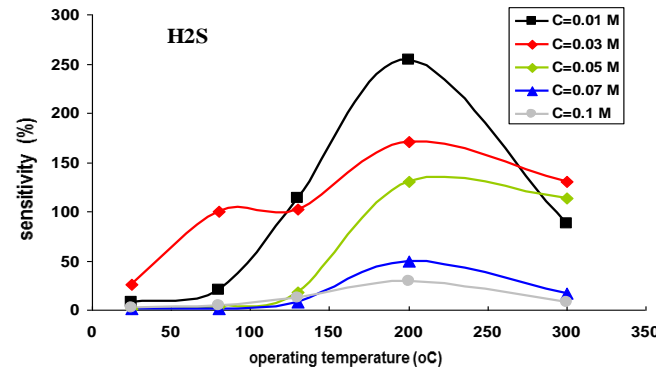
Figure 4. The variation of the sensitivity for H₂S gas with operating temperature at different concentrations.

The structural parameters such as (lattice constants (a), dislocation density (δ), mean strain (ε), and space factor(d)) of the spray-deposited NiO thin films have been calculated according to following equations [21-23], and the results are listed in Table 1.

$$n\lambda = 2d\sin\theta \tag{5}$$

$$d_{hkl} = \frac{a_{hkl}}{\sqrt{h^{\Upsilon} + k^{\Upsilon} + l^{\Upsilon}}} , \tag{6}$$

$$\varepsilon = \frac{a_{exp} - a_{bulk}}{a_{bulk}} , \tag{7}$$

$$\delta = \frac{\Lambda}{D^{\Upsilon}} \left(lines / m^{\Upsilon} \right), \tag{8}$$

hkl represents Miller indices.

The values of lattice parameters (for all samples) are smaller than thier analogous for a NiO standard bulk lattice (a=4.17382 Å). This decreasing of lattice parameters values can be explanted as the change in lattice parameter due to an internal strain, defects and dislocations in the films, there are similar results have been published by other researchers [24, 25].

The change in the lattice parameter values as appear in table 1 spatially in the angle 2Θ=37.5° is may be due to the shift in Bragg angle and so the corresponding interplanar spacing (d_{hkl} Å).

It is also worth noting, the appearance of the negative sign in the mean strain equation indicate that, the strain is a compressive.

The average of crystals size has been estimated by use the reliable peaks, and that shown the crystals enlarges from 10.67 nm to 28.53 nm with increasing of the solution concentration from 0.01M to 0.1 M.

This can be explained due to the presence of impurities and their impact on the structure and size of crystallite. Additionally, films that have the best structural properties characterizes by smallest mean strain value [24, 25].

Atomic force microscope has been used to study the surface properties in terms of roughness, images are shown in figure 3. The analysis of these results revealed a uniform distribution of grains, with grain size increasing as concentration increases the grains size was in range of 42.04-110.058 nm.

The roughness and average grain size values are estimated and listed in Table 2. The results of this study are consistent with those of M. Dharani Devi et al. [26].

3.2. Gas sensor measurements

Figure 4 shows that the responsivity to (5%) hydrogen sulfide gas rises when the operating temperature increase, and reach the optimum performance at ~200 ℃ temperature.

Also as shown in the figure 4, when the operating temperature exceeds the optimum temperature (~200 ℃) the sensitivity decrease. The highest response of the sensor was 254% at concentration 0.01 M, which is not different from the results of similar researches, as reported M.M. Gomaa et al. [27].

The response of a metal oxide gas sensor to the presence of a given gas depends on the speed of the chemical reaction on the surface of the grains and the speed of diffusion of the gas molecules to that surface which are activation processes and the activation energy of the chemical reaction is higher.

The gas sensor response is affected by several factors such as the thickness of the film, grain size and porosity. Smaller grain size tends to increase the response of the sensor, which is attributed to the large active surface for sensing because of high surface-volume ratio [28].

Figure 5 shows that the measurements of times for response and a recover of different operating temperature appearance that the both times of the sensor decreases with increasing operating temperature at which the lowest response time and best recovery time of the sensor about 2.68.sec and 75.6sec respectively at operating temperature 200 oC for concentration 0.03M.
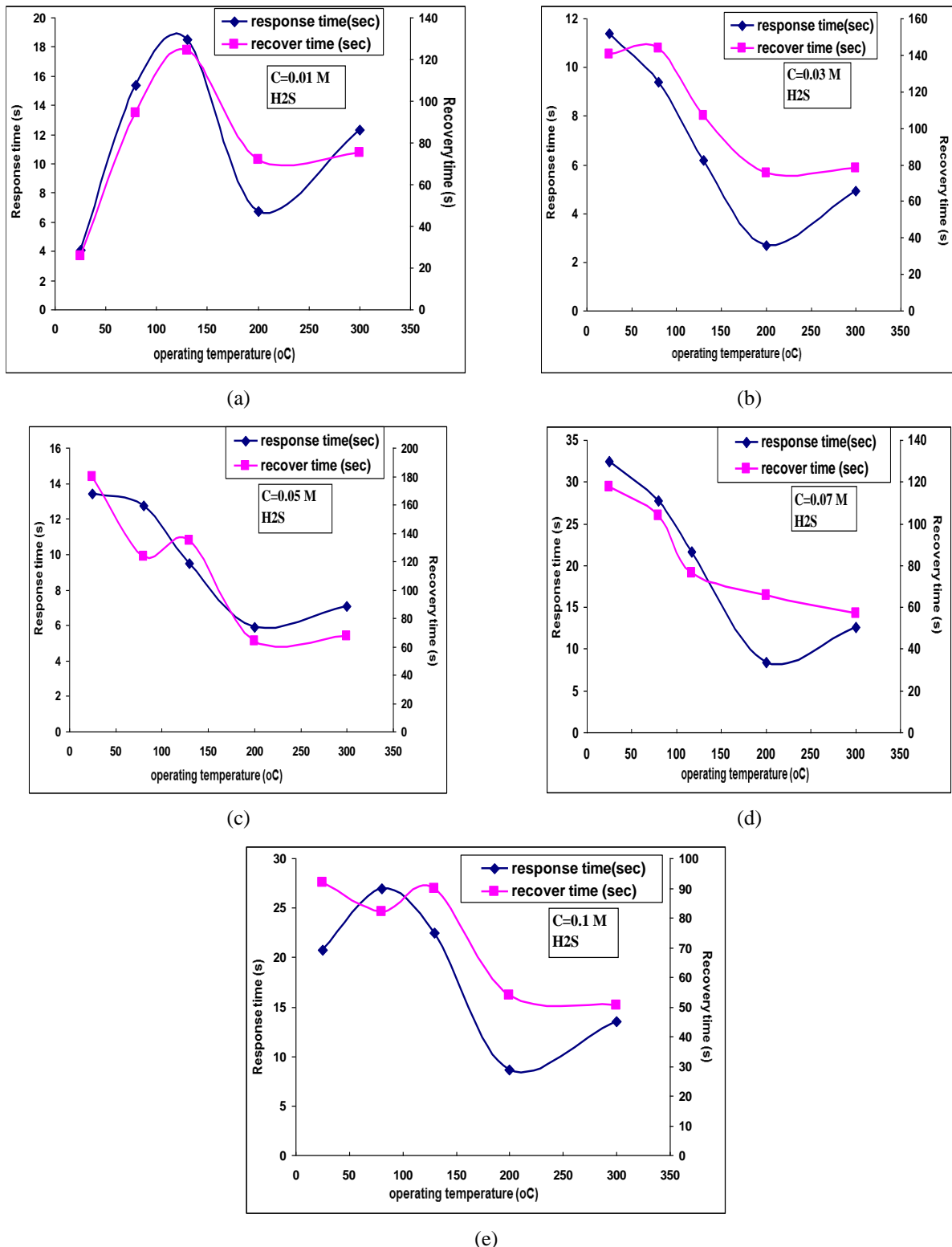
(a)

(b)

(c)

(d)

(e)

Fgure 5. The variation of Response and Recovery times with operating temperature at difference concentrations (a:0.01, b: 0.03,.c:0.05, d:0.07 and e: 0.1M)

It is true that the response to 0.01Mconcentration is greater than the response to 0.03M concentration, but the important thing is that the response time to the last concentration is much less than the 0.01M concentration. The results of the present report were summarized in Table 3.

The response times as mentioned above depended on crystallite size in which at the low concentration as shown in XRD and AFM results. And so decrease the thickness of the film may be a suitable method to improve the response time

As a result, the optimum performance includes a high sensitivity of 171 % and a faster response time for this system, which was achieved by using a sample prepared

at a concentration of 0.03 M at operating temperature about 200 ℃.

4. Conclusion

The utilize of spray pyrolysis technique to fabricate detect hydrogen sulfide thin film with thickness varies between 250 to 300 nm has been successfully studied. The structural of the produced films were characterized by X-ray diffraction, and atomic force microscopic. The x-ray data has confirmed the films have a FCC crystalline structure, and the size of the crystallites were ranged from 10.67 to 28.53 nm.

While atom force microscope images shows that the surface morphology of the spray-deposited NiO thin films have granular structure with a rough surface. The results of the gas-sensing show that NiO thin films created with 0.03 M concentration have a higher sensitivity to detect H_2S gas than NiO sensors prepared with higher concentrations.

References

1. I Hotovy , V Rehacek, M Kemeny, P Ondrejka, I Kostic, M. Mikolasek , and L Spiess, *Journal of Electrical Engineering* **72**, 1 (2021) 61.
2. P S Patil and L D Kadam, *Applied Surface Science* **199** (2002) 211.
3. I Hotovy, V Rehacek, P Siciliano, S Capone, and L Spiess, *Thin solid films* **418** (2002) 9.
4. S Palanichamya, J Raj Mohamedb, K Deva, Kumarc, P S Satheesh Kumara, S Pandiarajand, and L Amalraj, *Optik*, **194** (2019) 162887.
5. Y S Amir and J M Abass, *International Letters of Chemistry, Physics and Astronomy* **13** (2013) 90.
6. J Zhang, Z Qin, D Zeng, and C Xei , *Phys. Chem. Chem. Phys*. **19** (2017) 6313.
7. M GhouAli S, "*Elaboration and characterization of nanostructuring NiO thin films for gas sensing applications*", Doctoral Thesis, Biskra University, Algeria (2019) 38.
8. Y ZhO, H Wang, C Wu, Z F Shi, F B Gao, W C Li, G G Wu, B L Zhang, and G T Du, *Vacuum* **103** (2014) 14.
9. A M Soleimanpour, M Amir Jayatissa, and H Ahalapitiya, *Applied Surface Science* **276** (2013) 291.
10. D Y Jianga, J M Qina, X Wangb, S Gaoa, A C Lianga, and J X Zhaoa, *Vacuum* **86**, 8 (2012) 1083.
11. V Julijana, P G Margareta, N Metodija, and S Nace, *Silpakorn University Science and Technology Journal* **5**, 1 (2011) 34.
12. J H Ahmed, *Journal of Modern Physics* **5** (2014) 2184.
13. L Sang, Guogang Xu, Zhiwei Chen, Xinzhen Wang, Hongzhi Cui, Gaoyu Zhang, Yajie Dou, *Materials Science in Semiconductor Processing* **105** (2020) 104710.
14. P Shankar and J B B Rayappan, *Science Letters Journal* **126**, 4 (2015) 1.
15. Radhyah M Aljarrah, *Journal of Physics: Conference Series*. **1279**, 1 (2019) 012064.
16. Sharma, Bharat, and Jae-ha Myung, *Ceramics International* **46** (2020) 11.
17. Radhyah M Aljarrah and A M Aljawdah, *Materials Science Forum* **1039** (2021) 416.
18. Radhyah M Aljarrah and I M Alessa, *International Journal of Energy and Environment* **10**, 3 (2019) 163.
19. A S Garde, *International Journal of Chemical and Physical Sciences* **5**, 3 (2016) 1.
20. D Callister, "Materials science and engineering an introduction", John Wiley and Sons, New York , (1997) 174.
21. C Ricbard Brundle Charles A Evans, Jr., Sbaun Wihon, and Lee E Fitzpatrick, "Encyclopedia of Materials Characterization: Surfaces, Interfaces, Thin Films", Publishing by Butterworth- Heinemann, a division of Reed CUSA Inc (1992).
22. Y Shao, D Tang, J Sun, Y Lee, and W Xiong, China Part. **2** (2004) 119.
23. John J Quinn and Kyung-Soo Yi, "*Solid State Physics Principles and Modern Applications*", Springer-Verlag Berlin Heidelberg, (2009).
24. R Barir, B Benhaoua, S Benhamida, A Rahal, T Sahraoui, and R Gheriani, *Journal of Nanomaterials* (2017) 1.
25. S Joishy, and B V Rajendra, *Journal of Electronic Materials* **47**, 11 (2018) 6681.
26. M Dharani Devi, A Vimala Juliet, K Hariprasad, V Ganesh, H Elhosiny Ali, H Algarni, and I S Yahia, *Materials Science in Semiconductor Processing* **127** (2021) 105673.
27. M M Gomaa, M H Sayed, V L Patilb, M Boshta, and P S Patil, *Journal of Alloys and Compounds* **885** (2021) 160908.
28. M Kandyla , C Chatzimanolis-Moustakasa, M Guziewiczb, and M Kompitsas, *Materials Letters* **119** (2014) 51.